Current Biology 20, 909–913, May 25, 2010 ©2010 Elsevier Ltd All rights reserved DOI 10.1016/j.cub.2010.03.058

Report

Contribution of Inferior Temporal and Posterior Parietal Activity to Three-Dimensional Shape Perception

Bram-Ernst Verhoef,[1] Rufin Vogels,[1] and Peter Janssen[1,*]
[1]Laboratorium voor Neuro- en Psychofysiologie, Campus Gasthuisberg, O&N2, Herestraat 49, Bus 1021, BE 3000 Leuven, Belgium

Summary

One of the fundamental goals of neuroscience is to understand how perception arises from the activity of neurons in the brain [1]. Stereopsis is a type of three-dimensional (3D) perception that relies on two slightly different projections of the world onto the retinas of the two eyes, i.e., binocular disparity. Neurons selective for curved surfaces defined by binocular disparity may contribute to the perception of an object's 3D structure. Such neurons have been observed in both the anterior lower bank of the superior temporal sulcus (TEs, part of the inferior temporal cortex [IT]) and the anterior intraparietal area (AIP; [2–4]). However, the specific contributions of IT and AIP to depth perception remain unknown. We simultaneously recorded multiunit activity in IT and AIP while monkeys discriminated between concave and convex 3D shapes. We observed a correlation between the neural activity and behavioral choice that arose early and during perceptual decision formation in IT but later and after perceptual decision formation in AIP. These results suggest a role for IT, but not AIP, in 3D shape discrimination. Furthermore, the results demonstrate that similar neuronal stimulus selectivities in two areas do not imply a similar function.

Results and Discussion

Monkeys were trained to discriminate between concave and convex 3D shapes with, as operant, a saccade to one of two response targets that appeared immediately after stimulus presentation (Figure 1A). In each trial, a static random-dot stereogram portraying either a concave or a convex surface was presented at one of three positions in depth, i.e., in front of, behind, or at the fixation plane. This procedure enforces the use of perceptual strategies that are based on disparity variations within the stimulus (i.e., disparity gradients or curvature) rather than strategies relying on position-in-depth information (i.e., near or far decisions; see Supplemental Results available online). Task difficulty was manipulated by varying the signal strength of the stimulus, i.e., the percentage of dots defining the 3D surface (see Experimental Procedures). Average performance for the 100% signal strength stimuli ranged from 97% to 99% correct and decreased as a function of the signal strength of the stimulus (see Figure S1 for the performance at different positions in depth).

Although the stimulus duration was fixed in our 3D shape discrimination task and the animals were allowed to respond only after stimulus offset, we were able to estimate the monkey's average decision time by virtue of small but consistent deviations of the average eye position relative to baseline fixation during stimulus presentation. The time at which the mean horizontal eye traces, sorted according to the two pending choice directions (i.e., left or right saccade), started to diverge indicates a commitment toward a perceptual decision and can therefore be used as an estimate of the monkey's average "decision time" (Figures 2A and 2D). We used receiver operating characteristic (ROC) analysis to estimate this decision time. The ROC analysis indicates how well an ideal observer would predict the upcoming response (i.e., convex versus concave choice) with the eye position averaged in 20 ms long bins of a single trial. The decision time is estimated as the time at which the ROC value is significantly larger than 0.5 (see Experimental Procedures). For 0% signal strength, the average decision time was 270 ms and 415 ms for monkeys B1 and B2, respectively (green arrow in Figure 2). As expected, for the 100% signal strength condition, the decision time was shorter: 210 ms and 400 ms for monkeys B1 and B2, respectively (black arrow in Figure 2). We examined the validity of these decision time estimates by testing both monkeys with a stimulus duration of 270 ms (n = 5 sessions). For this short stimulus duration, the behavioral performance at 100% signal strength was similar to the performance obtained for the standard 800 ms duration (Figures 2C–2F). At lower signal strengths, performance was reduced, especially in monkey B2, as might be expected from his longer decision time with the standard stimulus duration. Note that the decision time estimates represent an upper bound on the true decision time (see Figure S2 for further validation).

To assess trial-to-trial correlations between the neural activity in inferior temporal cortex (IT) and anterior intraparietal area (AIP) and the behavioral response of the animal, we calculated choice probabilities (CP; [5–8]; see Experimental Procedures). For each 3D-shape selective site (41 in IT; 51 in AIP; see Experimental Procedures), CPs were calculated for each combination of signal strength, 3D shape, and position in depth, with at least seven responses to each choice target. The multiunit activity (MUA) displayed similar selectivity for concave versus convex 3D shapes in both areas (AIP versus IT selectivity: $p > 0.05$, based on 100% signal strength stimuli; see Experimental Procedures; see also Figure S3), although the latency of this selectivity was shorter in AIP (monkey B1: 110 ms; monkey B2: 100 ms) compared to IT (monkey B1: 120 ms; monkey B2: 120 ms). Because the average CPs were virtually identical across signal strengths and 3D shapes ($p > 0.05$ in all monkeys and both areas; permutation t test; see Supplemental Results), we combined the data of different stimulus conditions to obtain a single grand CP for each 3D-shape selective site (see Experimental Procedures).

The time courses of the average CPs differed conspicuously in the two areas (Figure 3): significant CPs arose earlier in IT than in AIP, despite the earlier 3D shape selectivity in AIP. The IT-CPs were already present at 100–140 ms after stimulus onset. However, the average CP in AIP increased at a point much later in time: for both monkeys, the average AIP-CP increased after the average IT-CP had reached its peak. Importantly, the average IT-CP was significantly elevated before each monkey overtly displayed its choice, whereas the average AIP-CP started to increase only after the animal had indicated

*Correspondence: peter.janssen@med.kuleuven.be

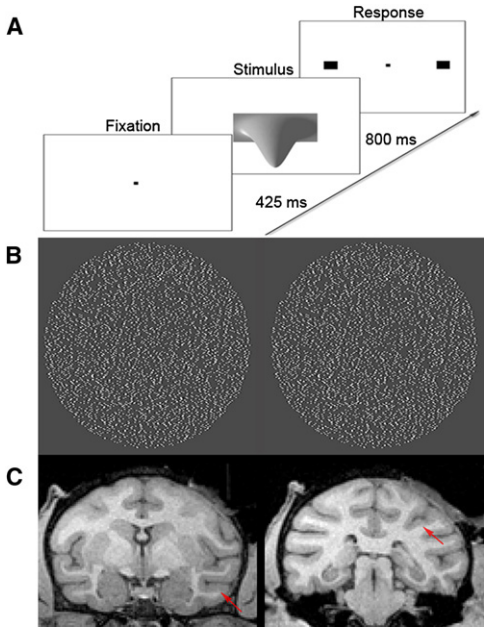

Figure 1. Task, Stimuli, and Recording Positions

(A) Trial sequence: trials started with 425 ms fixation (fixation window < 1.5° on a side) followed by 800 ms stimulus presentation. If the monkey maintained his gaze within the fixation window throughout the whole stimulus presentation, two response targets appeared on the left and right side of the fixation dot at 6° eccentricity. The subject was required to make a saccade to one of these targets depending on whether he perceived a convex (to the right or left for monkeys B2 and B1, respectively) or concave (to the left or right for monkeys B2 and B1, respectively) shape. Correct answers were followed by a liquid reward. The monkeys were rewarded randomly on the 0% signal strength trials with a probability of 0.5.

(B) Example of a convex random-dot stereogram positioned at the fixation plane at 100% signal strength.

(C) Estimated recording positions in the lower bank of the superior temporal sulcus (TEs) (left) and anterior intraparietal area (AIP) (right), indicated by a red arrow on a structural MRI.

its choice. In the stimulus period before the estimated decision time of each monkey, we observed a significant average IT-CP in both animals (monkey B1: average IT-CP = 0.55 in [100 ms, 270 ms]; n = 28 MUA sites; above 0.5, $p < 0.001$; monkey B2: average IT-CP = 0.54 in [100 ms, 415 ms]; n = 13 MUA sites; above 0.5, $p < 0.001$; bootstrap t test). Importantly, no significant average AIP-CP was observed in the predecision time period (monkey B1: average AIP-CP = 0.51; monkey B2: average AIP-CP = 0.51; not above 0.5, $p > 0.05$; bootstrap t test). After the estimated decision time, however, we did observe a significant average AIP-CP in both monkeys. For monkey B1, the AIP-CP started to increase around 270 ms after stimulus onset and resulted in a significant average AIP-CP of 0.64 in the [270 ms, 800 ms] interval (n = 37 MUA sites; above 0.5, $p < 0.001$; bootstrap t test). For monkey B2, the average AIP-CP started to increase just before stimulus offset, i.e., around 790 ms, and resulted in a significant average AIP-CP of 0.57 in the [790 ms, 1000 ms] interval (above 0.5, $p = 0.02$; n = 14 MUA sites; bootstrap t test). For monkey B2, we observed no significant AIP-CP in the [415 ms, 800 ms] interval (average AIP-CP = 0.52; $p > 0.05$). In monkey B1—but not in B2—the MUA selectivity correlated significantly with the CP of the MUA site during the predecision period in IT and during the postdecision period in AIP (IT: $r = 0.46$, $p = 0.015$; AIP: $r = 0.64$, $p < 0.001$). The observed CPs were not caused by random disparity fluctuations in the low signal strength stimuli or by vergence or other eye movements (Supplemental Results).

In principle, the fast 3D-shape selective responses of AIP neurons could be used to form perceptual decisions about disparity-defined 3D shapes [4]. So what, then, might explain the observed differences between the CPs in these two areas? First, the CPs of IT and AIP were measured in the same hemisphere of each subject and in the same recording sessions for each subject. This design excludes task strategy, lateralization, and learning effects as possible explanations for the observed CP difference between both areas [9, 10]. Second, the use of MUA for the calculation of CPs is appropriate in the context of our "coarse" stereopsis task [11–13], but MUA-CPs are sensitive to the amount of clustering shown by selective cells in an area. However, the degree of MUA selectivity was similar in both areas. Moreover, in agreement with previous studies [4, 14], we observed similar degrees of single-unit 3D shape selectivity in both areas (measured during a fixation task; $p > 0.05$ for a difference in 3D shape selectivity; 67 AIP cells, 59 IT cells; Supplemental Results). Hence, the similar MUA selectivity of both areas was not caused by weak clustering of highly selective single units in one area and strong clustering of weakly selective single units in the other area. Therefore, no differences in clustering of 3D-shape selective cells were found between both areas. Third, a difference in the noise correlation between two populations involved in perceptual decisions has been suggested as an important factor in determining the magnitude of the CPs [15, 16]. Hence, a lower noise correlation in AIP could have resulted in a lower CP because CPs calculated on the MUA most likely reflect such correlations [11]. However, we did observe significant CPs in AIP, but only after the subject had formed its decision. Because it seems unlikely that the AIP-CPs resulted from variability in the eye movements of the monkeys (Supplemental Results), they seem to have arisen from top-down influences. Such late, presumably top-down-driven CPs have been reported in several visual areas [17–19].

Although the interpretation of CPs can be a thorny issue [18], the observed time course of the IT-CP is at least compatible with IT participating in the perception of disparity-defined curved surfaces. Indeed, lesions to IT degrade performance on a global stereopsis task in both monkeys [20] and human subjects [21]. In contrast, evidence for posterior parietal cortex playing any causal role in stereo perception is scarce [21]. One study reported a variable deficit in the discrimination of the 3D orientation of large planar surfaces after muscimol injection in area CIP [22]. To our knowledge, however, no study has investigated the role of posterior parietal cortex in a global stereopsis task with shape as the discriminandum. Because reversible inactivation of AIP results in grasping deficits [23] and stereoinformation is important for proper grasping [24–26], it is highly likely that the stereoinformation in AIP is used for grasping purposes rather than for perception [24, 25].

In summary, we observed a significant covariation between the neural activity of area TEs, which is part of IT, and the behavioral response of the subject during 3D shape discrimination. Several independent observations suggest that the CP in TEs occurred during the formation of perceptual decisions regarding 3D shapes. First, the CP emerged about 100–140 ms after stimulus onset and declined toward the end of the stimulus presentation. Second, analysis of eye movements during stimulus fixation indicated that the animals became overtly committed to a particular choice after the onset of the CP in IT. Hence, the formation of perceptual

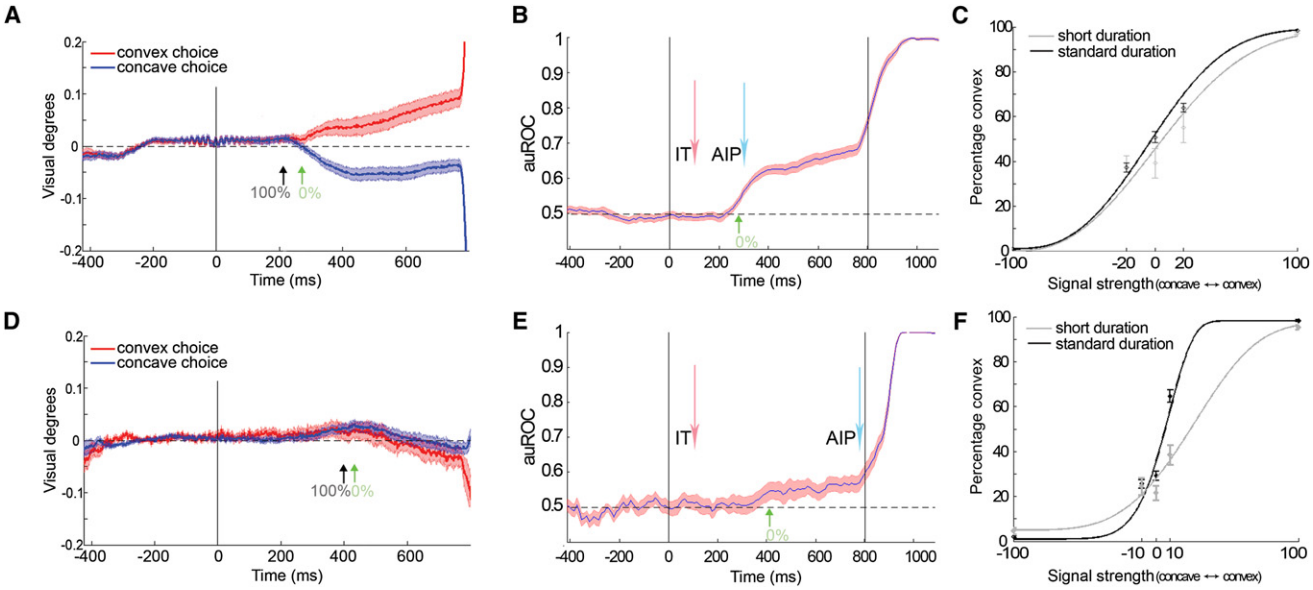

Figure 2. Estimated Decision Time

(A–E) Average horizontal eye position during the course of the trial for monkey B1 (A) and monkey B2 (D) for the 0% signal strength trials. Red and blue lines plot the average horizontal eye positions in trials with a pending convex or concave choice, respectively. The black vertical line indicates stimulus onset and offset. The horizontal dashed line indicates baseline fixation. Standard error of the mean (SEM) (±) at each time point is indicated by shading over the lines. The brisk change in the eye position around 800 ms corresponds to the initiation of the saccadic response. The time course of the receiver operating characteristic (ROC) values (20 ms bins) is shown in (B) and (E) for monkeys B1 and B2, respectively. These ROC time courses are related to (A) and (D) but provide a sensitive measure of the degree to which the eye positions predict the convex or concave target choice on a single trial. The green (270 ms and 415 ms for monkeys B1 and B2, respectively) and black (210 ms and 400 ms for monkeys B1 and B2, respectively) arrows indicate the time of significant eye position divergence between the two average eye traces for the 0% and 100% signal strength trials, respectively (based on the ROC analysis). For comparison, the red and blue arrows indicate the latency of the average IT-CPs and AIP-CPs, respectively (inferior temporal cortex [IT]: 140 ms; AIP: 300 ms for monkey B1 and 790 ms for monkey B2).

(C and F) Percentage of convex choices as a function of the signal strength for the stimuli with normal (i.e., 800 ms; black) and short (i.e., 270 ms; gray) stimulus durations for monkey B1 (C) and monkey B2 (F). The behavioral performance of monkey B1 dropped with 6% at 20% signal strength (64% correct versus 58% correct; d'-difference between short and long stimulus duration at 20% signal strength = 0.27). In contrast, the behavioral performance of monkey B1 dropped with 13% at 10% signal strength (70% correct versus 57% correct; d'-difference = 0.67). Vertical lines indicate ±1 SEM. Solid line shows the fitted psychometric function. Psychometric functions were fitted to the monkeys' average performance at different signal strengths with a cumulative Weibull function via maximum likelihood estimation [31].

decisions regarding 3D shapes was initiated shortly after stimulus onset, i.e., during the time that IT-CPs occurred. In contrast, the AIP-CP occurred much later and after perceptual decisions about 3D shapes were already formed. These results suggest a role for IT, but not AIP, in 3D shape discrimination. Hence, our findings are consistent with the view that the dorsal stream is important for using visual information to effect actions, whereas the ventral visual stream underlies perception and object recognition [27, 28]. More generally, our results clearly demonstrate that similar neuronal stimulus selectivities in two areas do not imply a similar function.

Experimental Procedures

Subjects and Surgery

Two monkeys (*Macaca mulatta*) served as subjects. Under isoflurane anesthesia and aseptic conditions, a recording cylinder (Thomas Recording) was implanted above the intraparietal sulcus and anterior IT (left and right hemispheres for monkeys B1 and B2). All surgical procedures and animal care were approved by the K.U. Leuven Ethical Committee and were in accordance with the European Communities Council Directive 86/609/EEC.

Stimuli

The stimulus set consisted of static random-dot stereograms with eight different circumference shapes (e.g., circle, ellipse, square, etc.; size = ~5°). We first selected the optimal circumference shape via a fixation task in which only 100% signal strength stimuli were presented. The preferred circumference shape, as determined in one of the two regions (varied daily), was subsequently used during the discrimination task. Stimuli were centered foveally on a gray background. The depth structure was defined solely by horizontal disparity as a two-dimensional radial basis Gaussian surface that could be either convex or concave (see Figure 1B for an example stimulus; maximal disparity amplitude = 0.15°). The dots consisted of Gaussian luminance profiles (width = 7 pixels; height = 1 pixel; standard deviation = 0.7 pixels; 1 pixel ≈ 0.02°). For each dot, the mean of the Gaussian luminance profile could be positioned along a continuous axis resulting in perceptually smooth stereograms with subpixel resolution [29]. Stimuli were presented at three positions in depth, i.e., in front of, behind, or at the fixation plane (±0.23° depth variation). Task difficulty was manipulated by varying the percentage of dots defining the surface, i.e., the signal strength (or stereocoherence). Dots that were not designated as defining the surface were assigned a disparity that was randomly drawn from a uniform distribution (support = [−0.50°, 0.50°]). During recording, we used three different signal strengths (0%, 20%, and 100% for monkey B1; 0%, 10%, and 100% for monkey B2). For each experiment we used 20 different random dot patterns per signal strength (see Supplemental Experimental Procedures for additional information).

Data Analysis

To estimate the monkeys' average decision time, we analyzed the deviations from baseline fixation in the average horizontal eye traces. For each trial, the eye movement traces were normalized by subtraction of the average fixation position of the baseline period. We used only the eye movement data from trials for which CPs were calculated. For each site, the left and right eye traces were sorted according to the two pending choice

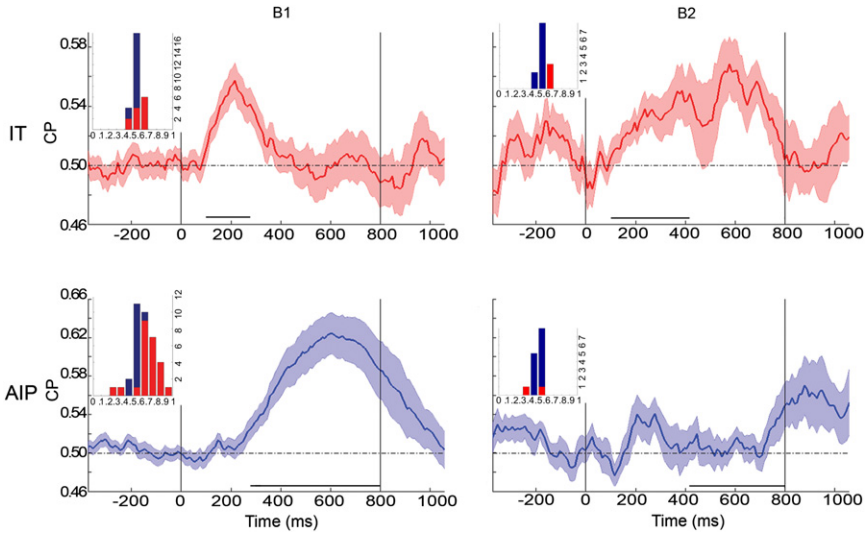

Figure 3. Grand Choice Probability as a Function of Time

We examined the time course of the grand choice probability (CP) via a sliding window analysis in which the grand CP was calculated for the neural data contained in a 100 ms time window (centered at 50 ms) that was advanced in time in steps of 10 ms. This procedure was repeated for each 3D-shape selective site, and all time courses were then averaged for each region separately. Black vertical lines indicate stimulus onset and offset.

Top: average IT grand CPs. Bottom: average AIP grand CPs. Left: monkey B1. Right: monkey B2. Insets display the distributions of the grand CPs for all 3D selective sites for each monkey and each area separately, based on the time interval as shown by the black line at the bottom of each plot. This time interval is the predecision time interval for IT and the postdecision time interval for AIP (see Results and Discussion). Red bars indicate the sites with a CP that is significantly different from chance. Horizontal dashed lines indicate chance level. SEM (±) at each time point is indicated by shading over the lines.

directions (i.e., left or right saccade) and averaged per choice direction. Next, we calculated, for each site and each choice direction, the average of these mean left and right eye traces (Figures 2A and 2D). Single-trial horizontal eye positions were used to calculate a time course of ROC values (i.e., the area under the ROC curve; auROC). ROC values were calculated for the horizontal eye position averaged within 20 ms bins. The ROC time courses were subsequently averaged across sites. The "decision time" was estimated as the first of three consecutive 20 ms bins for which the ROC value differed significantly from chance (bootstrap test, $\alpha = 0.05$).

3D shape selectivity was examined for trials with stimuli at 100% signal strength via a two-way analysis of variance with "3D shape" and "position in depth" as factors based on the 700 ms interval starting 100 ms after stimulus onset. 3D shape selectivity was defined as a significant main effect of 3D shape ($\alpha = 0.05$). The "preferred 3D shape" of a 3D-shape selective site was defined as the depth profile (i.e., convex or concave) with the highest average response in the 700 ms interval. We compared the degree of 3D shape selectivity in AIP and IT by calculating ROC values on the MUA (averaged within different time intervals, i.e., pre- or postdecision; Figure S3) for the preferred and the nonpreferred 100% signal strength stimuli. We did this for each site that was used to calculate CPs. We used a permutation test to compare the ROC values of each region. We calculated the selectivity latency for each region as follows. First, for each site, a peristimulus-time histogram (PSTH) (10 ms bins) was calculated for the preferred and the nonpreferred 100% signal strength stimulus. Second, the PSTHs were normalized with the maximum bin value of any PSTH at a given site and were averaged across sites. Third, the selectivity latency was defined as the first of two consecutive bins, for which we observed a significant difference between the preferred and the nonpreferred stimulus (paired permutation t test over sites; $\alpha = 0.05$). Choice probabilities were calculated for each combination of signal strength, 3D shape, and position in depth [30]. For each 3D-shape selective site, the CP was tested for a significant deviation from 0.5 via a permutation test ($\alpha = 0.05$). Grand CPs were obtained for each 3D-shape selective site by first Z-scoring the neural data within each condition (with ≥ 7 trials per choice target; no 100% signal strength conditions) and subsequently combining the Z-scored data of different conditions to calculate the grand CP.

Supplemental Information

Supplemental Information includes Supplemental Results, Supplemental Experimental Procedures, three figures, and two tables and can be found with this article online at doi:10.1016/j.cub.2010.03.058.

Acknowledgments

We thank I. Puttemans, P. Kayenbergh, G. Meulemans, S. Verstraeten, M. Docx, T. Frank, H. Seynnaeve, W. Depuydt, and M. De Paep for assistance. We thank S. Raiguel for comments on a previous version of this manuscript. This work was supported by Neuroprobes (EU project IST-027017), Fonds voor Wetenschappelijk Onderzoek grants G.0495.05N and G.0713.09, Geneeskundige Stichting Koningin Elisabeth, Interuniversitaire Attractiepolen P6/29-C, Geconcertreerde Onderzoeks Acties grant 2005/18, Human Frontiers Science Program Career Development Award 0057/2005-C, and Excellentiefinanciering grant 05/014.

Received: December 22, 2009
Revised: March 12, 2010
Accepted: March 12, 2010
Published online: April 29, 2010

References

1. Parker, A.J., and Newsome, W.T. (1998). Sense and the single neuron: Probing the physiology of perception. Annu. Rev. Neurosci. *21*, 227–277.
2. Janssen, P., Vogels, R., and Orban, G.A. (2000). Selectivity for 3D shape that reveals distinct areas within macaque inferior temporal cortex. Science *288*, 2054–2056.
3. Janssen, P., Vogels, R., Liu, Y., and Orban, G.A. (2001). Macaque inferior temporal neurons are selective for three-dimensional boundaries and surfaces. J. Neurosci. *21*, 9419–9429.
4. Srivastava, S., Orban, G.A., De Mazière, P.A., and Janssen, P. (2009). A distinct representation of three-dimensional shape in macaque anterior intraparietal area: Fast, metric, and coarse. J. Neurosci. *29*, 10613–10626.
5. Nienborg, H., and Cumming, B.G. (2006). Macaque V2 neurons, but not V1 neurons, show choice-related activity. J. Neurosci. *26*, 9567–9578.
6. Nienborg, H., and Cumming, B.G. (2007). Psychophysically measured task strategy for disparity discrimination is reflected in V2 neurons. Nat. Neurosci. *10*, 1608–1614.
7. Uka, T., and DeAngelis, G.C. (2004). Contribution of area MT to stereoscopic depth perception: Choice-related response modulations reflect task strategy. Neuron *42*, 297–310.
8. Uka, T., and DeAngelis, G.C. (2006). Linking neural representation to function in stereoscopic depth perception: Roles of the middle temporal area in coarse versus fine disparity discrimination. J. Neurosci. *26*, 6791–6802.
9. Chowdhury, S.A., and DeAngelis, G.C. (2008). Fine discrimination training alters the causal contribution of macaque area MT to depth perception. Neuron *60*, 367–377.
10. Hamsher, K.D. (1978). Stereopsis and unilateral brain disease. Invest. Ophthalmol. Vis. Sci. *17*, 336–343.

11. Liu, J., and Newsome, W.T. (2005). Correlation between speed perception and neural activity in the middle temporal visual area. J. Neurosci. *25*, 711–722.
12. Liu, J., and Newsome, W.T. (2006). Local field potential in cortical area MT: Stimulus tuning and behavioral correlations. J. Neurosci. *26*, 7779–7790.
13. Purushothaman, G., and Bradley, D.C. (2005). Neural population code for fine perceptual decisions in area MT. Nat. Neurosci. *8*, 99–106.
14. Janssen, P., Vogels, R., and Orban, G.A. (1999). Macaque inferior temporal neurons are selective for disparity-defined three-dimensional shapes. Proc. Natl. Acad. Sci. USA *96*, 8217–8222.
15. Cohen, M.R., and Newsome, W.T. (2009). Estimates of the contribution of single neurons to perception depend on timescale and noise correlation. J. Neurosci. *29*, 6635–6648.
16. Shadlen, M.N., Britten, K.H., Newsome, W.T., and Movshon, J.A. (1996). A computational analysis of the relationship between neuronal and behavioral responses to visual motion. J. Neurosci. *16*, 1486–1510.
17. Dodd, J.V., Krug, K., Cumming, B.G., and Parker, A.J. (2001). Perceptually bistable three-dimensional figures evoke high choice probabilities in cortical area MT. J. Neurosci. *21*, 4809–4821.
18. Nienborg, H., and Cumming, B.G. (2009). Decision-related activity in sensory neurons reflects more than a neuron's causal effect. Nature *459*, 89–92.
19. Uka, T., Tanabe, S., Watanabe, M., and Fujita, I. (2005). Neural correlates of fine depth discrimination in monkey inferior temporal cortex. J. Neurosci. *25*, 10796–10802.
20. Cowey, A., and Porter, J. (1979). Brain damage and global stereopsis. Proc. R. Soc. Lond. B Biol. Sci *204*, 399–407.
21. Ptito, A., Zatorre, R.J., Larson, W.L., and Tosoni, C. (1991). Stereopsis after unilateral anterior temporal lobectomy. Dissociation between local and global measures. Brain *114*, 1323–1333.
22. Tsutsui, K., Jiang, M., Yara, K., Sakata, H., and Taira, M. (2001). Integration of perspective and disparity cues in surface-orientation-selective neurons of area CIP. J. Neurophysiol. *86*, 2856–2867.
23. Gallese, V., Murata, A., Kaseda, M., Niki, N., and Sakata, H. (1994). Deficit of hand preshaping after muscimol injection in monkey parietal cortex. Neuroreport *5*, 1525–1529.
24. Marotta, J.J., Behrmann, M., and Goodale, M.A. (1997). The removal of binocular cues disrupts the calibration of grasping in patients with visual form agnosia. Exp. Brain Res. *116*, 113–121.
25. Murata, A., Gallese, V., Luppino, G., Kaseda, M., and Sakata, H. (2000). Selectivity for the shape, size, and orientation of objects for grasping in neurons of monkey parietal area AIP. J. Neurophysiol. *83*, 2580–2601.
26. Watt, S.J., and Bradshaw, M.F. (2002). Binocular information in the control of prehensile movements in multiple-object scenes. Spat. Vis. *15*, 141–155.
27. Goodale, M.A., Milner, A.D., Jakobson, L.S., and Carey, D.P. (1991). A neurological dissociation between perceiving objects and grasping them. Nature *349*, 154–156.
28. Orban, G.A., Janssen, P., and Vogels, R. (2006). Extracting 3D structure from disparity. Trends Neurosci. *29*, 466–473.
29. Bach, M., Schmitt, C., Kromeier, M., and Kommerell, G. (2001). The Freiburg stereoacuity test: Automatic measurement of stereo threshold. Graefes Arch. Clin. Exp. Ophthalmol. *239*, 562–566.
30. Britten, K.H., Newsome, W.T., Shadlen, M.N., Celebrini, S., and Movshon, J.A. (1996). A relationship between behavioral choice and the visual responses of neurons in macaque MT. Vis. Neurosci. *13*, 87–100.
31. Wichmann, F.A., and Hill, N.J. (2001). The psychometric function: I. Fitting, sampling, and goodness of fit. Percept. Psychophys. *63*, 1293–1313.